Zeitschrift: Eclogae Geologicae Helvetiae
Herausgeber: Schweizerische Geologische Gesellschaft
Band: 71 (1978)
Heft: 2

Artikel: The rheological behavour of polycrystalline anhydrite
Autor: Müller, Walter H. / Briegel, Ueli
DOI: https://doi.org/10.5169/seals-164739

Eclogae geol. Helv.	Vol. 71/2	Pages 397-407	7 figures in the text and 1 table	Basle, July 1978

The rheological behaviour of polycrystalline anhydrite[1])

By WALTER H. MÜLLER and UELI BRIEGEL[2])

ABSTRACT

Fine-grained anhydrite from Riburg (Switzerland) was investigated under a confining pressure of 1.5 kbar (150 MPa) at temperatures ranging from 20 to 450 °C and at strain rates of 10^{-4} down to 10^{-7}sec^{-1}. A number of relaxation tests permitted extrapolation to even lower strain rates. The strength (at 10% strain) varied from 4.15 kbar ($T=20$ °C; $\dot{\varepsilon}=8.5\cdot10^{-5}\text{sec}^{-1}$) to 505 bar ($T=450$ °C; $\dot{\varepsilon}=7.1\cdot10^{-7}\text{sec}^{-1}$). Work hardening was effective at low temperatures and fast strain rates and resulted in a strength higher than 1.3 kbar, whereas at higher temperatures and slower strain rates, steady-state flow (at lower strength) was observed. The following flow law (GAROFALO 1965), first used for olivine by POST (1977) fits very well our observations:

$$\dot{\varepsilon}=A\cdot\exp\left(\frac{-H}{R\cdot T}\right)\cdot\left(\sinh\frac{\sigma}{\sigma_0}\right)^n.$$

For our anhydrite samples, the constants were empirically determined to be $A=2.07\cdot10^5\ \text{sec}^{-1}$, $H=36.39\pm2.24\ \text{kcal}\cdot\text{mol}^{-1}$, $\sigma_0=800$ bar and $n=2$.

In view of the possible role of anhydrite as a decollement horizon at the base of overthrusts, a comparison of its strength with that of halite, of Solnhofen limestone and of Yule marble can be made. At low temperatures and fast strain rates, the strength of anhydrite is similar to the strength of Solnhofen limestone and higher than that of marble. However, the minimum temperature for a drastic reduction of the strength (at geological strain rates) is considerably lower for anhydrite than for the carbonates. The lowest temperature at which these rocks would favourably act as a decollement horizon are room temperature for halite, 180 °C for anhydrite and 350 °C for fine-grained limestones.

ZUSAMMENFASSUNG

Das Fliessverhalten von Anhydrit der Bohrung Riburg (NE Rheinfelden) wurde mittels Triaxialkompressions- und Relaxationstests bei einem konstanten Manteldruck von 1,5 kbar, in einem Temperaturbereich von 20 bis 450 °C und bei Verformungsraten von 10^{-4} bis $10^{-7}\,\text{sec}^{-1}$, untersucht. Die Festigkeitswerte, bestimmt jeweils bei 10% Verformung, variieren zwischen 4,15 kbar bei Raumtemperatur und einer Verformungsrate ($\dot{\varepsilon}$) von $8{,}5\cdot10^{-5}\text{sec}^{-1}$ und 505 bar ($T=450$ °C, $\dot{\varepsilon}=7{,}1\cdot10^{-7}\text{sec}^{-1}$). Übersteigt der Anhydrit eine Festigkeit von 1,3 kbar, d.h. bei tiefen Temperaturen und schnellen Deformationsraten, zeigen die Spannungs-/Verformungskurven «work hardening». Bei höheren Temperaturen zeigt der Anhydrit Gleichgewichtsfliessen und erreicht nur noch geringere Festigkeitswerte. Mit dem folgenden Fliessgesetz (GAROFALO 1965), welches erstmals von POST (1977) für Olivin angewandt wurde, konnten unsere Anhydritdaten sehr gut dargestellt werden:

$$\dot{\varepsilon}=A\cdot\exp\left(\frac{-H}{R\cdot T}\right)\cdot\left(\sinh\frac{\sigma}{\sigma_0}\right)^n.$$

Für die Konstanten wurden folgende Daten ermittelt: $A=2{,}07\cdot10^5\,\text{sec}^{-1}$, $H=36{,}39\pm2{,}24\,\text{kcal}\cdot\text{mol}^{-1}$, $\sigma_0=800$ bar und $n=2$.

---

[1]) Contribution No. 127 of the Laboratory of Experimental Geology, ETH, Zürich (Switzerland).

[2]) Geological Institute, Swiss Federal Institute of Technology, Zürich (Switzerland).

Im Hinblick auf Abscherungs- und Überschiebungshorizonte wurden Steinsalz, Anhydrit, Solnhofener Kalk und Yule-Marmor untereinander verglichen. Dabei zeigte sich, dass unter allen Umständen Steinsalz die besten Voraussetzungen mitbringt. Bei Raumtemperatur und schnellen Verformungsraten zeigen Anhydrit und Solnhofener Kalk sehr ähnliche, hohe Festigkeiten (um 4 kbar), Yule-Marmor etwas weniger. Wird die Temperatur nun erhöht, wird zuerst Anhydrit, dann Marnor und zuletzt der Kalk seine Festigkeit drastisch verringern. Die Bedingungen für einen Abscherungshorizont sind für Steinsalz bei Raumtemperatur, für Anhydrit von 180 °C an und bei Solnhofener Kalk von 350 °C an gegeben. Die Festigkeitsreduktion bei Marmor ist weniger ausgeprägt. Marmor würde erst bei sehr hohen Temperaturen den Bedingungen genügen.

Introduction

It is well-known from field observations, that evaporites play an important role in tectonic processes. Evaporite layers can serve as detachment surfaces and lead to the development of complicated tectonic structures. It is therefore of great interest to know more on the flow behaviour of such rocks. Halite has been investigated thoroughly by HEARD (1972). Deformation experiments on anhydrite under high confining pressures and elevated temperatures have been made and reported by HANDIN & HAGER (1957, 1958), MÜLLER & SIEMENS (1974) and MÜLLER & BRIEGEL (1977), but there had been no flow law established for anhydrite deformation.

All our specimens were deformed in compression under a confining pressure of 1.5 kbar (150 MPa), using a triaxial deformation apparatus. Techniques and apparatus are described in MÜLLER & BRIEGEL (1977). The rock samples were taken from cores from a drillhole near Riburg, in the Swiss "Tafeljura" (Hole No. 51, Schweizerische Rheinsalinen). It is a very pure (> 90% $CaSO_4$) and fine-grained anhydrite. Thin-section studies revealed a very felted texture of anhydrite needles with an average length of 0.3 mm and an average diameter of 0.05 mm. Cylindrical specimens used in experiments were 12 mm in diameter and 24 mm long, cored perpendicular to bedding.

Experimental results

Constant strain rate tests

A summary of all our experiments is compiled in the Table (strength at 10% strain). Figures 1 to 4 show stress/strain curves at different temperatures (300–450 °C). Deformation at 300 °C or lower temperatures takes place with distinct work hardening. Steady-state flow occurs during deformation at 350 °C with strain rates of about $10^{-6}\,sec^{-1}$ and at higher temperature with faster strain rates.

The strength under steady-state conditions is always below 1.3 kbar.

Stress relaxation tests

Stress relaxation data can be obtained after each successful constant strain rate test. The motor drive is stopped and the stress drop is recorded as a function of time. The stress, corresponding to the elastic energy stored in the sample and in the apparatus, is "relaxed", e.g. some of the elastic deformation of sample and

Table: *Deformation tests on polycrystalline anhydrite at 1.5 kbar confining pressure.* (R = stress relaxation tests)

Experiment Nr	Temperature °C	Differential stress at 10% strain	Strain rate sec^{-1}
48 R	20	4148	$8{,}5.10^{-5}$
49	20	4022	$8{,}2.10^{-6}$
52 R	300	3331	$8{,}1.10^{-6}$
53 R	300	4062	$8{,}0.10^{-5}$
54 R	300	4068	$4{,}2.10^{-5}$
56 R	300	3754	$1{,}9.10^{-5}$
57	300	3680	$1{,}1.10^{-5}$
59	300	3192	$5{,}2.10^{-6}$
60	300	3090	$1{,}5\text{-}10^{-6}$
74 R	350	3790	$8{,}4.10^{-5}$
75 R	350	3310	$4{,}2.10^{-5}$
76 R	350	3108	$1{,}9.10^{-5}$
77	350	2475	$8{,}3.10^{-6}$
79 R	350	1696	$7{,}7.10^{-7}$
80	350	1784	$1{,}5.10^{-6}$
81 R	350	2124	$3{,}4.10^{-6}$
38	400	2789	$8{,}3.10^{-5}$
39	400	2705	$6{,}4.10^{-5}$
40	400	2031	$3{,}0.10^{-5}$
41	400	1971	$1{,}8.10^{-5}$
42	400	1838	$1{,}1.10^{-5}$
43	400	1870	$8{,}3.10^{-6}$
44	400	1645	$6{,}2.10^{-6}$
45	400	1349	$3{,}8.10^{-6}$
46	400	982	$1{,}7.10^{-6}$
62 R	400	2422	$3{,}0.10^{-5}$
72	400	(5,3%) 754	$7{,}0.10^{-7}$
73 R	400	2347	$4{,}5.10^{-5}$
82 R	400	2573	$8{,}2.10^{-5}$
83 R	400	1468	$3{,}7.10^{-6}$
84 R	400	1198	$2{,}4.10^{-6}$
64 R	450	1981	$8{,}3.10^{-5}$
65	450	1635	$3{,}1.10^{-5}$
66 R	450	1185	$1{,}2.10^{-5}$
67 R	450	1092	$6{,}2.10^{-6}$
68 R	450	949	$3{,}7.10^{-6}$
69	450	(6,1%) 670	$1{,}6.10^{-6}$
70 R	450	684	$1{,}6.10^{-6}$
71	450	(3,1%) 505	$7{,}1.10^{-7}$

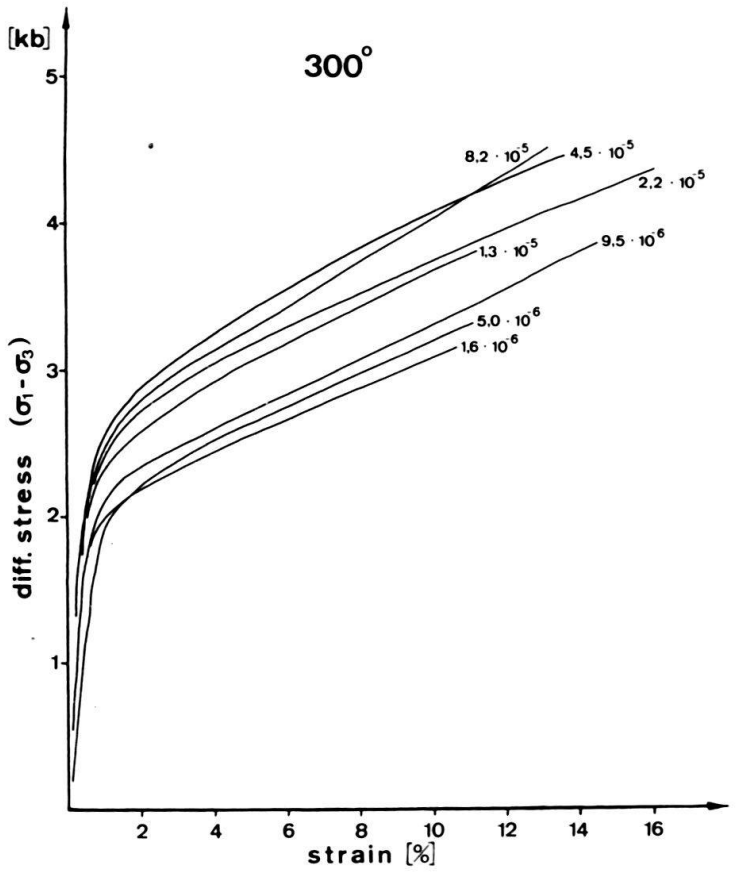

Fig. 1. Differential stress/strain curves for anhydrite compressed at 1.5 kbar confining pressure, $\dot{\varepsilon} = 8.2 \cdot 10^{-5}$ to $1.6 \cdot 10^{-6} \mathrm{sec}^{-1}$ and 300 °C.

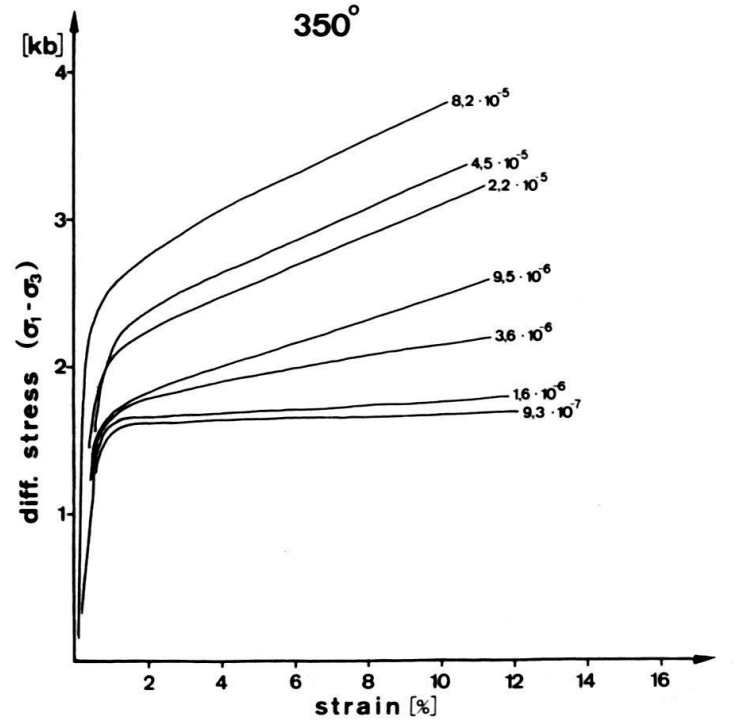

Fig. 2. Differential stress/strain curves for anhydrite compressed at 1.5 kbar confining pressure, $\dot{\varepsilon} = 8.2 \cdot 10^{-5}$ to $9.3 \cdot 10^{-7} \mathrm{sec}^{-1}$ and 350 °C.

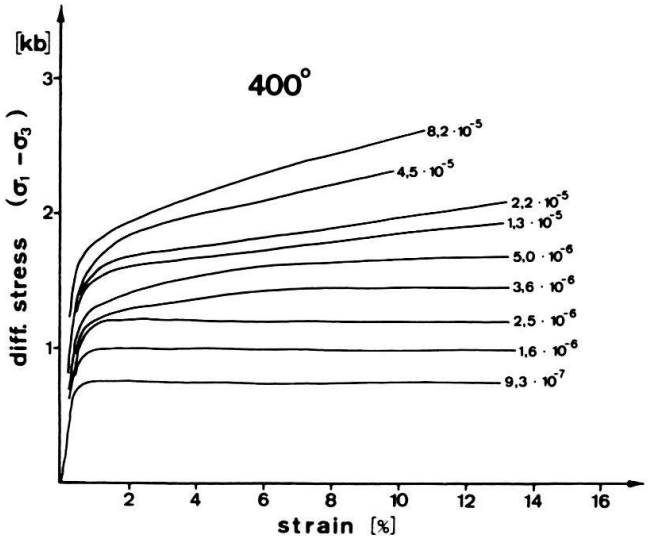

Fig. 3. Differential stress/strain curves for anhydrite compressed at 1.5 kbar confining pressure, $\dot{\varepsilon} = 8.2 \cdot 10^{-5}$ to $9.3 \cdot 10^{-7} \mathrm{sec}^{-1}$ and 400 °C.

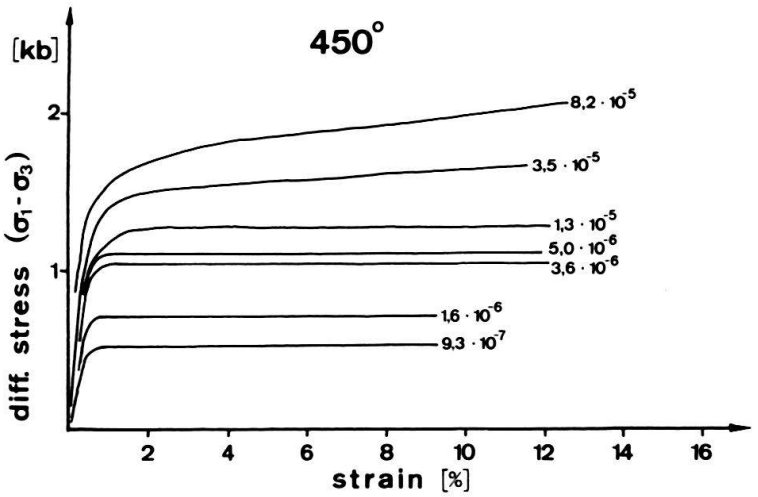

Fig. 4. Differential stress/strain curves for anhydrite compressed at 1.5 kbar confining pressure, $\dot{\varepsilon} = 8.2 \cdot 10^{-5}$ to $9.3 \cdot 10^{-7} \mathrm{sec}^{-1}$ and 450 °C.

apparatus is slowly converted into plastic deformation of the sample. This technique has been used already by RALEIGH & KIRBY (1970), RUTTER & SCHMID (1975) and SCHMID (1976). Such a stress-time curve covers a great range of different strain rates and differential stresses. The strain rates during relaxation are related to the observed "stress rate" $d\sigma/dt$ by equation

$$\dot{\varepsilon}_S = (L_a K_a + K_s) \cdot \frac{d\sigma}{dt}$$

where K_a and K_s are the compliances of apparatus and the samples and L_a is a constant relating the elastic apparatus distortion to the plastic deformation of the sample. The stress rate $(d\sigma/dt)$ can be readily taken from the stress-time plot as tangent to the stress relaxation curve. All three constants are determined in calibration runs. With this technique we are able to extend our data to the range

of strain rates down to $10^{-8}\,\mathrm{sec}^{-1}$. The results of these relaxation tests are presented in a double logarithmic stress/strain rate plot (Fig. 5). For every given temperature, except the room temperature, distinct sets of curves, each corresponding to a single relaxation experiment, can be drawn.

The flow law

In the region of thermally activated plastic flow, the pseudoviscous behaviour of a material can be described by the following equation (DORN 1957):

$$\dot{\varepsilon} = c \cdot \exp\left(\frac{-H}{R \cdot T}\right) \cdot f(\sigma) \tag{1}$$

where H is the apparent activation energy for creep, R = the gas constant and T the temperature in °K. $f(\sigma)$ describes the non-linear stress dependence of strain rate. It is clear from Figure 5 that $f(\sigma)$ must be a complex function, the strain rate does not follow the usual exponential stress-dependence $(\dot{\varepsilon} \propto \exp(\sigma/a))$ or the power law relationship $(\dot{\varepsilon} \propto \sigma^n)$. Before we determine the function $f(\sigma)$ it is easiest to first calculate the apparent activation energy H describing the temperature dependence of strain rate.

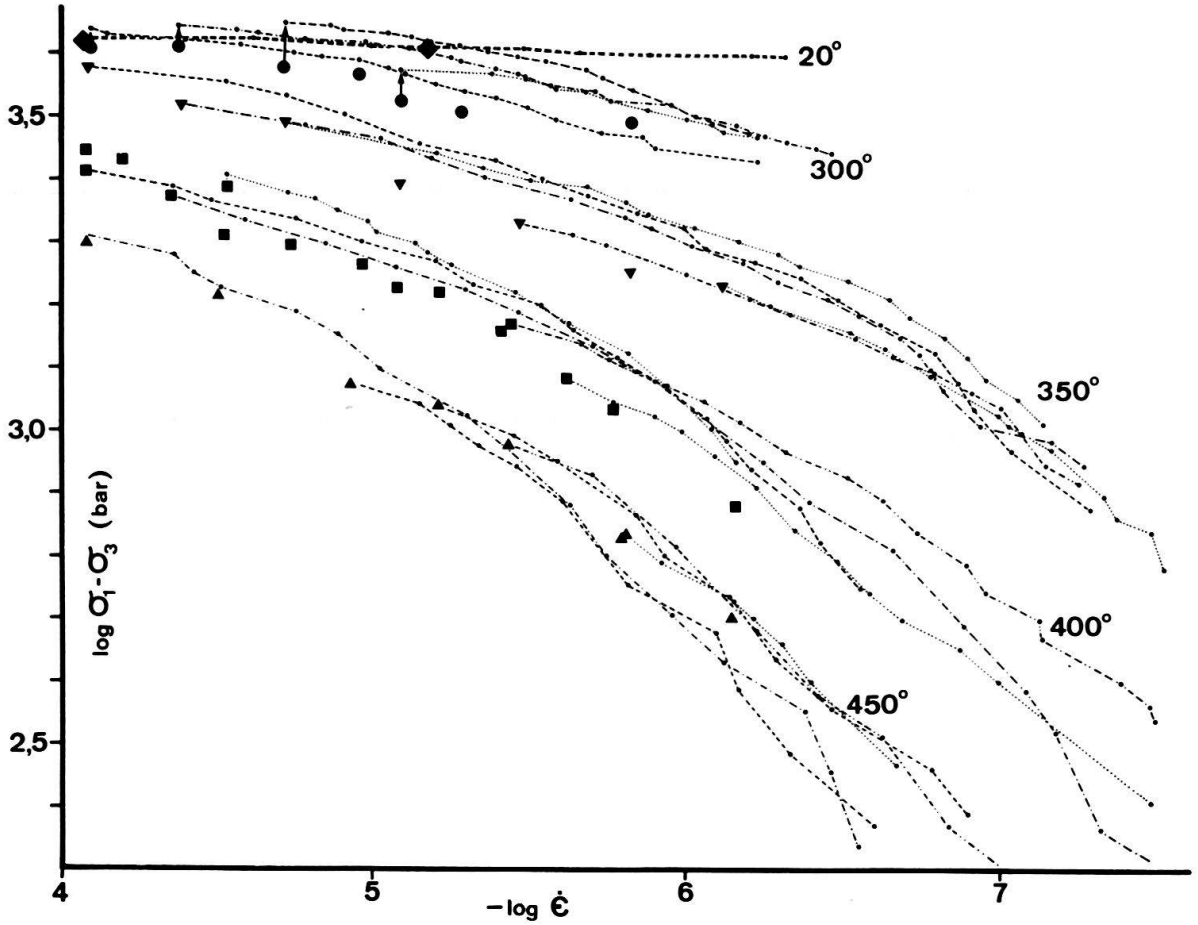

Fig. 5. Log$\dot{\varepsilon}$ vs. logσ diagram. Constant stress/strain data points corresponding to those listed in the Table are shown in fat symbols. Stress relaxation data points belonging to one relaxation test are interconnected by dashed/dotted lines.

Differentiating the logarithm of equation (1) with respect to $1/T$ at constant σ, we get

$$\left[\frac{\delta \log \dot{\varepsilon}}{\delta \frac{1}{T}}\right]_{\sigma} = \frac{-H \cdot \log e}{R}$$

and for a small ΔT, we can approximate this equation with

$$H = -R\,2.3 \cdot \left[\frac{\log \dot{\varepsilon}_{T_1} - \log \dot{\varepsilon}_{T_2}}{\frac{1}{T_1} - \frac{1}{T_2}}\right] \tag{2}$$

$1/\log e$ being 2.3.

Equation (2) now enables us to determine H from the difference in the logarithm of the strain rates at two given temperatures T_1 and T_2 at constant stress. Thus we determined H at small stress intervals ($\Delta \log \sigma = 0.05$) by taking the average strain rate at any given temperature and stress. Thereby we noted that H is not a function of stress and amounts to 36.4 ± 2.2 kcal · mol^{-1}. The data at 300 °C were omitted in the determination of H since we observed substantial work hardening under these conditions and because the specimens were relaxed at stresses much higher than that at 10% strain. At the higher temperatures all the relaxation tests were initiated at a stress similar to that at 10% strain.

All the data of Figure 5 have been normalized to a temperature of 300 °C in Figure 6, where black dots represent constant strain rate experiments (at 10% strain) and open circles represent stress relaxation values. The data points gather along a smoothly bent curve which tends to straighten out at the lowest stresses. The line

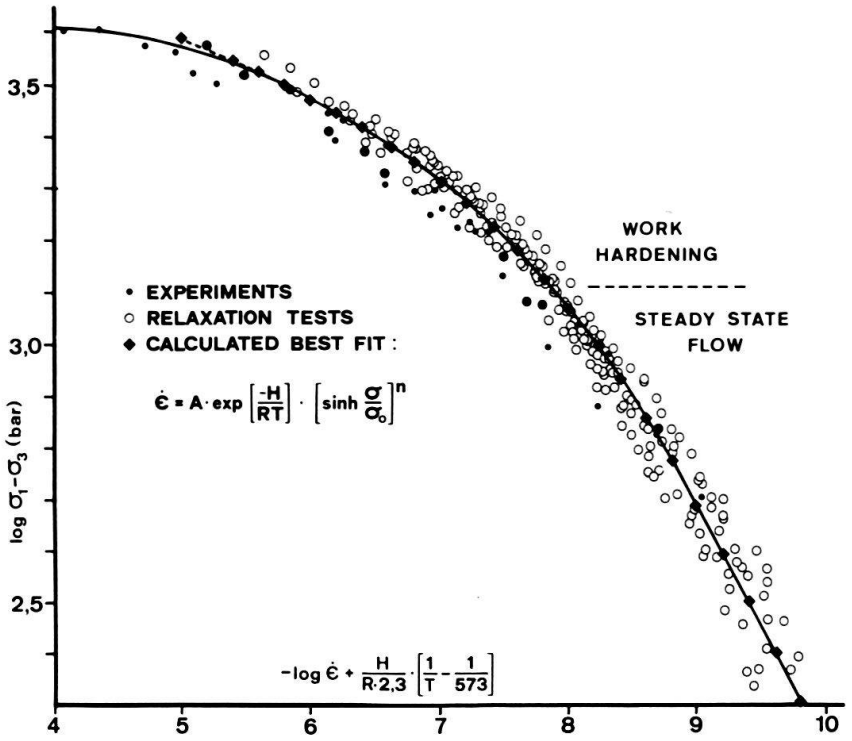

Fig. 6. Data of Figure 5 homologized to 300 °C. The black dots represent the constant strain rate results at 10% strain and the open circles the stress relaxation values.

shows that only the data in the lowest stress region could be adequately described by a power law relationship (equivalent to a straight line with a slope $1/n$ in Fig. 6) where

$$f(\sigma)=\sigma^n. \tag{3}$$

All the data in Figure 6 are best fitted to the complex function (solid line in Fig. 6)

$$f(\sigma)=c\cdot\left(\sinh\frac{\sigma}{\sigma_0}\right)^n \tag{4}$$

proposed by GAROFALO (1965), where c, σ_0 and n are constants. Equation (4) is well approximated by a simple power law relationship (equation 3) at stresses $\sigma/\sigma_0<0.7$ where $\sinh(\sigma/\sigma_0)\approx\sigma/\sigma_0$. At the higher stresses where $\sigma/\sigma_0>2$, equation (4) is approximated by the exponential stress dependence:

$$f(\sigma)=\exp\frac{\sigma}{a} \tag{5}$$

with $a=\sigma_0/n$ because $(\sinh(\sigma/\sigma_0))^n\approx 1/2^n\exp(\sigma_n/\sigma_0)$.

The stress dependence described by equation (4) corresponding to the solid line in Figure 6 can now be combined with the known activation energy to yield a complete flow law of the form

$$\dot{\varepsilon}=A\cdot\exp\frac{-H}{R\cdot T}\cdot\left(\sinh\frac{\sigma}{\sigma_0}\right)^n \tag{6}$$

and the following values for the constants have been calculated to fit our data on Riburg anhydrite:

$$A=2.07\cdot 10^5\,\mathrm{sec}^{-1}$$
$$H=36.4\pm 2.24\ \mathrm{kcal}\cdot\mathrm{mol}^{-1}=152.26\pm 9.37\ \mathrm{kJ}\cdot\mathrm{mol}^{-1}$$
$$\sigma_0=800\ \mathrm{bar}$$
$$n=2$$

As can be seen in Figure 6, our best fit line is good up to a differential stress of 3.3 kbar. At higher stresses we have strong work hardening, when the strength is highly dependent on confining pressure (MÜLLER & BRIEGEL 1977). This stress/strain relationship indicates that the dominant deformation mechanism is probably cataclastic flow.

Provisional microstructural investigations suggest that at stresses less than 3.3 kbar intracrystalline deformation mechanisms such as twinning and dislocation glide are the dominant deformation mechanisms.

In contrast to the observations on many other rock materials (CARTER 1976) deforming by dislocation creep, there is no region of constant n (equation 3) with a value between 3 and 8. There is apparently very little dislocation creep at intermediate stresses. Steady-state flow takes place at stresses below 1.3 kbar only (Fig. 1–4). Evaluation of equation (6) reveals that a region of constant n ($=2$) is reached below $\sigma/\sigma_0=0.7$, corresponding to stresses of less than 560 bar. In this low stress region the unusually low rate for n and the analogy to results of SCHMID (1976) and SCHMID et al. (1977) on fine-grained Solnhofen limestone suggests a deformation mechanism by grain boundary sliding. The activation energy is quite low with 36.4 kcal $\cdot$ mol^{-1}, compared to other available rock data (CARTER 1976) and only halite yields lower values (23.5 kcal $\cdot$ mol^{-1}; HEARD 1972).

Implications

Field observations have repeatedly indicated that evaporites (halite, gypsum and anhydrite) preferentially form detachment horizons at the base of overthrusts or disharmonic folds. A notable example is the deformation of the Mesozoic strata of the Jura mountains (BUXTORF 1916). We try now to evaluate the conditions ($\Delta\sigma$, T, $\dot{\varepsilon}$) under which anhydrite becomes mobile and to compare them to those of other well-known shear materials like halite (French Jura, Lons-le-Saunier; RICOUR 1956) and limestone (Glarus overthrust; SCHMID 1975).

For this purpose we compiled Figure 7 with the available data for Solnhofen limestone, Yule marble, anhydrite and halite. Unfortunately, the different authors applied different confining pressures and therefore we have had to omit data in the low temperature range where confining pressure is an important parameter. At 300 °C and $\dot{\varepsilon} = 10^{-5}\,\mathrm{sec}^{-1}$, our anhydrite has a similar strength to Solnhofen limestone ($\Delta\sigma > 4$ kbar) and exceeds the strength of Yule marble, whereas halite has a strength of only 500 bar at room temperature. We also see from Figure 7, that at a strain rate of $10^{-5}\,\mathrm{sec}^{-1}$, the Riburg anhydrite starts to decrease its strength at temperatures around 250 °C, Yule marble around 400 °C and Solnhofen limestone around 500 °C. We also would like to note the effect of grain size in carbonates: at low temperatures fine-grained Solnhofen limestone is appreciably stronger than Yule marble, however, with increasing temperature the curve for limestone falls well below that of marble (SCHMID 1976). Extrapolating the strain rate to geologically relevant values (between 10^{-10} and $10^{-14}\,\mathrm{sec}^{-1}$) we can readily determine from Figure 7 which rock would tend to yield first at any given temperature. Halite,

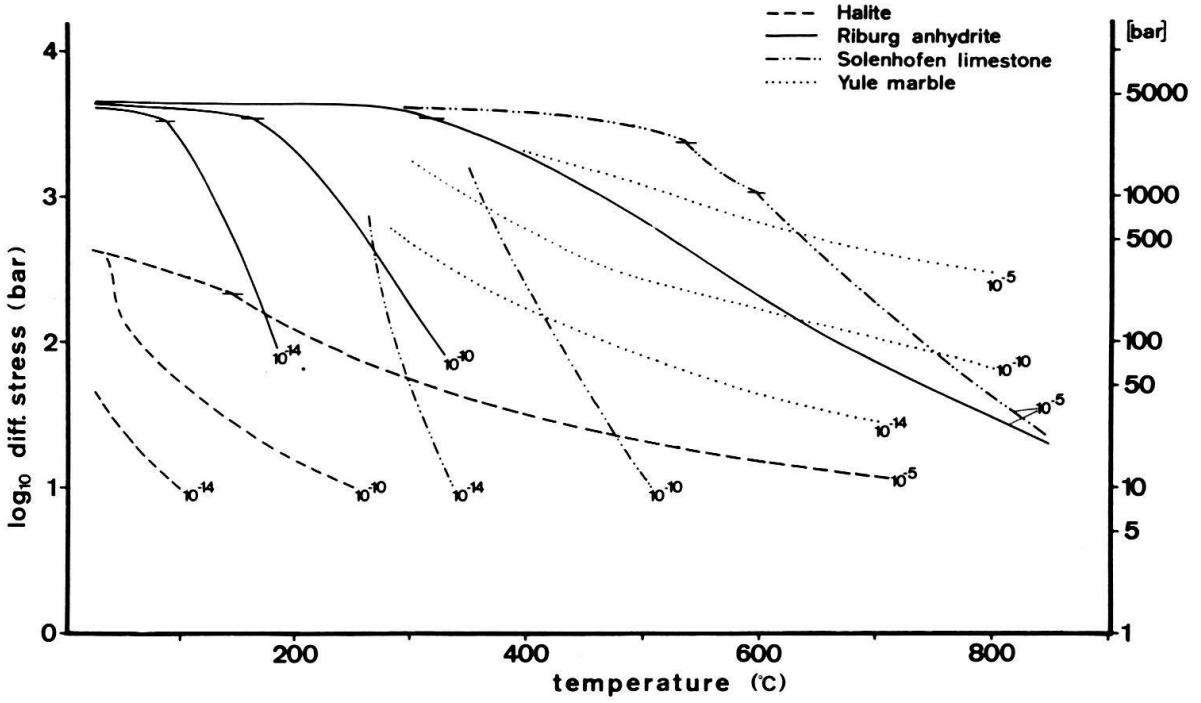

Fig. 7. A comparison between the rheological behaviour of halite (HEARD 1972), anhydrite, Solnhofen limestone (RUTTER 1974; SCHMID 1976) and Yule marble (HEARD & RALEIGH 1972) at different strain rates ($\dot{\varepsilon} = 10^{-5}$, 10^{-10} and $10^{-14}\,\mathrm{sec}^{-1}$).

whenever present, should act as the detachment horizon at all temperatures as its strength is minimal even at room temperature. Anhydrite yields preferentially in the absence of halite at temperatures above 180 or 220 °C depending upon strain rate. Solnhofen limestone, which may have a similar deformation behaviour as the Lochseiten limestone (the mylonite at the base of the Glarus overthrust) starts to flow at temperatures > 350 °C (at 10^{-10}sec^{-1} strain rate) (SCHMID 1975). It may then act as a decollement horizon if both halite and anhydrite are absent. Both carbonate rocks and anhydrite have a similar strength at low temperatures and fast strain rates. With increasing temperature and slow strain rate, however, they differ greatly in strength and ductility. Such a contrast is exhibited in the Belchen region of the Jura mountains: In a tunnel exposure ductile disharmonic folding of anhydrite is observed, whereas the limestone form large disharmonic folds, having been deformed by brittle fracture and to a very small extent by pressure solution (LAUBSCHER 1975).

Our experimental studies add valuable insight to the question of the mechanics of Jura deformation. LAUBSCHER (1961, 1967) already recognised the importance of evaporites as the detachment horizon under the Molasse basin and the Juras. There is no evidence of an extensive rock salt layer under the Molasse basin. Gypsum, unstable above 57 °C (HARDIE 1965), is probably not present in the decollement layer and in fact has not been detected in any drillhole so far.

Anhydrite is present ubiquitously under the Jura mountains and probably also underlies the Molasse basin SE of the Jura (TRÜMPY 1959). It seems to be a possible decollement horizon of the Jura folds. Our work on the deformation behaviour of anhydrite suggests that it might indeed yield by steady-state flow at relatively low temperature and low stress, if the strain rate is very slow. Work is now in progress on a new mechanical analysis of the Jura folding.

Acknowledgments

We would like to express our thanks to Prof. H. Jäckli, who initiated the project and to the NAGRA (Nationale Gesellschaft zur Lagerung radioaktiver Abfälle) for the supply of the sample material. We are very grateful to Prof. K.J. Hsü and Dr. S.M. Schmid for reading the manuscript and making useful suggestions. Mr. H. Naef provided laboratory assistance and drafted some of the figures.

REFERENCES

BUXTORF, A. (1916): *Prognosen und Befunde beim Hauensteinbasis- und Grenchenbergtunnel und die Bedeutung der letzteren für die Geologie des Juragebirges.* - Verh. natf. Ges. Basel *27,* 184–254.

CARTER, N.L. (1976): *Steady state flow of rocks.* - Rev. Geophys. Space Phys. *14,* 301–359.

DORN, J.E. (1957): *The spectrum of activation energies for creep.* In: *Creep and Recovery* (p. 255–283). - Amer. Soc. Metals (38th natl. metall. Congr. 1956, Cleveland, Ohio).

GAROFALO, F. (1965): *Fundamentals of creep and creep-rupture in metals.* - McMillan, New York.

HANDIN, J., & HAGER, R.V., Jr. (1957): *Experimental deformation of sedimentary rocks under confining pressure: Tests at room temperature on dry samples.* - Bull. amer. Assoc. Petroleum Geol. *41,* 1–50.

— (1958): *Experimental deformation of sedimentary rocks under confining pressure: Tests at high temperature.* - Bull. amer. Assoc. Petroleum Geol. *42,* 2892–2934.

HARDIE, L.A. (1965): *Gypsum-anhydrite equilibrium at 1 atm pressure.* - Spec. Pap. geol. Soc. Amer. *82,* 83-84.

HEARD, H.C. (1972): *Steady state flow in polycrystalline halite at pressure of 2 kilobars.* In: HEARD, H.C., BORG, I.V., CARTER, N.L., & RALEIGH, C.B. (Ed.): *Flow and Fracture of Rocks* (p. 191-210). - Geophys. Monogr. Ser. *16* (AGU, Washington, D.C.).

HEARD, H.C., & RALEIGH, C.B. (1972): *Steady state flow in marble at 500-800°C.* - Bull. geol. Soc. Amer. *83,* 935-956.

LAUBSCHER, H.P. (1961): *Die Fernschubhypothese der Jurafaltung.* - Eclogae geol. Helv. *54,* 221-282.

— (1967): *Geologie und Paläontologie: Tektonik.* - Verh. natf. Ges. Basel *78/1,* 24-34.

— (1975): *Viscous components in Jura folding.* - Tectonophysics *27,* 239-254.

MÜLLER, W.H., & BRIEGEL, U. (1977): *Experimentelle Untersuchungen an Anhydrit aus der Schweiz.* - Eclogae geol. Helv. *70/3,* 685-699.

MÜLLER, P., & SIEMENS, H. (1974): *Festigkeit, Verformbarkeit und Gefügeregelung von Anhydrit.* - Tectonophysics *23,* 105-127.

POST, L.R., Jr. (1977): *High temperature creep of Mt. Burnet Dunite.* - Tectonophysics *42,* 75-110.

RALEIGH, C.B., & KIRBY, S.H. (1970): *Creep in the Upper Mantle.* - Spec. Pap. mineral. Soc. Amer. *3,* 113-121.

RICOUR, J. (1956): *Le Chevauchement de la Bordure occidentale du Jura sur la Bresse dans la région de Lons-le-Saunier.* - Bull. Ver. schweiz. Petroleum-Geol. u. -Ing. *23/64,* 57-70.

RUTTER, E.H., & SCHMID, S.M. (1975): *Experimental study of unconfined flow of Solnhofen limestone at 500°-600°C.* - Bull. geol. Soc. Amer. *86,* 145-152.

SCHMID, S.M. (1975): *The Glarus Overthrust: Field evidence and mechanical model.* - Eclogae geol. Helv. *68,* 251-284.

— (1976): *Rheological evidence for changes in the deformation mechanism of Solnhofen limestone towards low stresses.* - Tectonophysics *31,* T21-28.

SCHMID, S.M., BOLAND, J.N., & PATERSON, M.S. (1977): *Superplastic flow in fine-grained limestone.* - Tectonophysics *43,* 257-291.

TRÜMPY, R. (1959): *Hypothesen über die Ausbildung von Trias, Lias und Dogger im Untergrund des schweizerischen Molassebeckens.* - Eclogae geol. Helv. *52/2,* 435-448.